

## STRUCTURAL ASSESSEMENT OF A STONE MASONRY WALL USING A CONTINUUM DAMAGE MODEL AND EXPERIMENTAL VALIDATION

Bruno Silva<sup>1</sup>, João Miranda Guedes<sup>2</sup>, António Arêde<sup>3</sup>, Aníbal Costa<sup>4</sup>

<sup>1</sup> Faculdade de Engenharia da Universidade do Porto  
Rua Dr. Roberto Frias s/n, 4200-465 Porto, Portugal  
e-mail: [brunoqsilva@hotmail.com](mailto:brunoqsilva@hotmail.com)

<sup>2/3</sup> Faculdade de Engenharia da Universidade do Porto  
Rua Dr. Roberto Frias s/n, 4200-465 Porto, Portugal  
e-mail: [jguedes@fe.up.pt](mailto:jguedes@fe.up.pt) / [aarede@fe.up.pt](mailto:aarede@fe.up.pt)

<sup>4</sup> Universidade de Aveiro  
Campus Universitário de Santiago, 3810-193 Aveiro, Portugal  
e-mail: [acosta@civil.ua.pt](mailto:acosta@civil.ua.pt)

**Keywords:** Masonry, cyclic load, experimental tests, numerical analysis, damage model homogeneous.

**Abstract.** *Understanding how stone masonry structures behave under dynamic horizontal loads yields important information on possible collapse mechanisms and damage progression along the structure. With this in mind a numerical and experimental study was performed concerning the structural behaviour of a stone masonry wall built in situ at the Laboratory of Seismic and Structural Engineering (LESE). The wall was tested under cyclic horizontal load to simulate the effects of a horizontal seismic action. The experimental response allowed assessing the cyclic behaviour and estimating the energy dissipation and ductility capacity of the structure, as well as its strength and stiffness. Afterwards, the wall was simulated numerically in Cast3M [1] using a finite element modelling strategy. The stones, the infill and the joints were simulated considering them as part of a unique homogeneous material and using a non-linear continuum damage model [2] to reproduce the wall's global behaviour.*

*The final objective of this work is to study the applicability of such continuum numerical models to simulate stone masonry structures, using experimental results as reference values.*

## 1 INTRODUCTION

The numerical simulation of a stone masonry structure, being made of multiple materials connected together with joints, is not an easy task. In most cases the structure is made of two leaves masonry walls filled with mortar of poor cohesion and strength materials.

Some authors have simulated the different materials of a masonry structure [7, 8]. Modelling the stones and the infill separately, introducing joint elements along the line dividing the two materials. This type of simulation usually considers different models for the different materials, concentrating the non-linear behaviour in the joint elements. The infill is not simulated and no voids are considered between the stones. Even with these simplifications, the dimension and shape of the stones must be known with some accuracy. If the wall is covered with mortar, it should be removed to enable access to the stone dimensions. Furthermore, the stones and the joints mechanical characteristics should be determined through in-situ or laboratory tests or based on properties from other works where structures with similar characteristics were tested or analysed. When the masonry is made of irregular stones, the simulation becomes even more difficult.

In order to overcome most of these problems, a non-linear continuum damage model [2] was selected to simulate stone masonry structures in a global homogeneous way. In order to have a measure of comparison to assess the viability of the model, an irregular stone masonry wall was built and tested at the Laboratory of Seismic and Structural Engineering (LESE) of the Faculty of Engineering of Porto University. The test was then simulated numerically using the referred model implemented in Cast3M [6] to verify its ability to reproduce the wall's behaviour. The wall was tested under constant vertical force and in-plane horizontal cyclic controlled displacements. Characteristics such as energy dissipation and ductility capacity of the wall, as well as its strength and stiffness were analysed and used as reference values to validate the continuum damage model.

The work presented herein is divided into 3 parts: the experimental test, the numerical simulation and the validation/calibration of the numerical model. The main conclusions are presented at the end of the paper.

## 2 THE EXPERIMENTAL TEST

Using the potentialities of the LESE, an irregular stone masonry wall was built and tested under constant vertical force and in-plane horizontal cyclic controlled displacements. This experiment allowed assessing the wall's behaviour and its main characteristics, such as energy dissipation, stiffness and strength.

The tested wall is a granite two leaves irregular masonry. The wall is a 1,6m long, 1,6m high and 0,6m thick. The two leaves are made of good quality granite stones. The stones were positioned in layers along both sides/leaves of the wall using clay mortar in between the stones. Furthermore, some of the stones were positioned along the transverse direction of the wall in order to connect the leaves and improve the wall's global behaviour. It should be noted that this is a reliable construction procedure commonly used on multiple leaves masonry structures (Figure 1).

The wall was built in side a  $1.6 \times 2.6 \times 0.6 \text{ m}^3$  concrete ring in order to simulate a rigid foundation.



Figure 1: The stone masonry wall specimen.

## 2.1 Test-setup

The wall was submitted to a constant vertical load of 50kN and to controlled horizontal in-plane cyclic displacements. The horizontal load was applied to the top of the wall through a hydraulic jack with hinges at the edges and using a steel reaction structure. To guarantee a uniform distribution of the load at the top, the two opposite lateral faces of the wall were connected using steel rods, as illustrated in Figure 2. The vertical force was applied to the top of the wall by means of two smaller hydraulic jacks. Each one was set against a steel beam connected to the concrete block through two steel rods. The foundation block was connected to the laboratory reaction floor via four monitored high strength pre-stressed rods in order to minimize displacements of the block during the test.

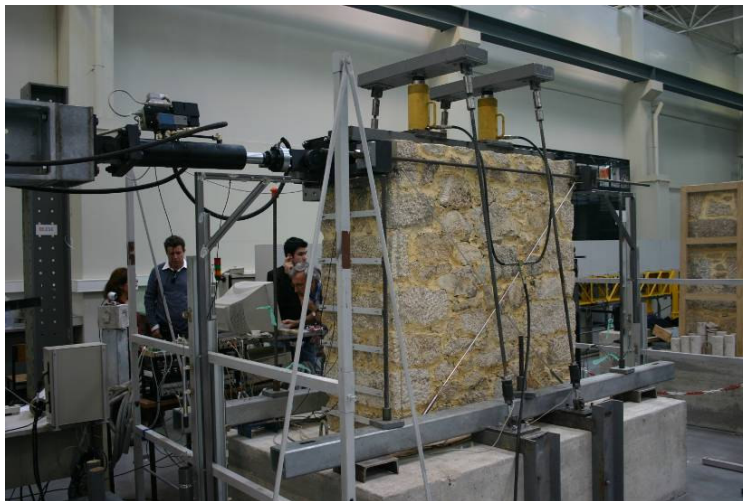


Figure 2: Wall test-setup.

The experimental test was performed using a displacement control system that simultaneously acquired data from all monitored spots. The wall was monitored using nine load cells (one at each of the four steel rods transferring the vertical reaction to the foundation block,

one at each of the four steel rods connecting the foundation block to the laboratory floor and one at the horizontal actuator) and twenty nine LVDT's, located as illustrated in Figure 3. The LVDT's numbers 01, 02, 03, 09, 10, 11, 18, 17, 19, 21, 25, 26, 27 and 14 are positioned between two contiguous stone blocks and allowed measuring the vertical movements of the lateral joints. The LVDT's 08, 06, 32, 33, 41, 23, 22, 31, 30 and 40 measured the horizontal displacements along the lateral facades; LVDT's 28 and 29 measured the displacements along the two diagonals of the main facade and 35 and 36 the displacements along the transversal direction of the wall. Figure 3 also indicates the positive direction of the horizontal displacements. LVDT 40 refers to the transducer that controls the actuator.

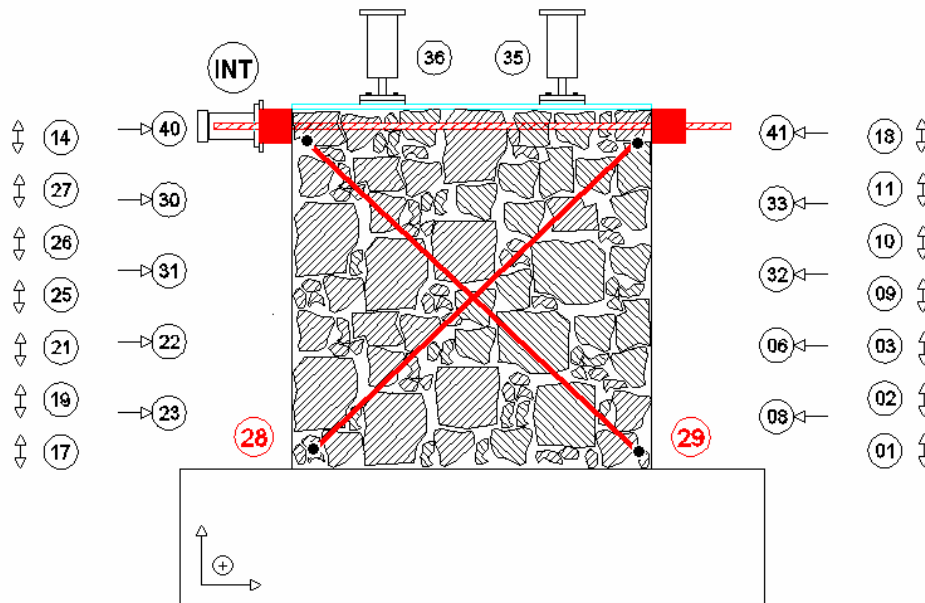


Figure 3: LVDT's setup.

## 2.2 Loading conditions

Besides self-weight, the wall was submitted to a constant vertical load of 50 kN and to controlled horizontal in-plane cyclic displacements, both applied at the top. The vertical load meant to simulate the existence of other structures/loads above being supported by the wall. The history of the horizontal displacements imposed on the in-plane direction at the top of the wall consisted of loading/unloading cycles with peaks ranging from 0 to 12 mm (Figure 4).

During the experimental test the steel rods connecting the two opposite lateral faces of the wall at the top suffered a loss of tension that caused the steel structure at the top of the wall to slide and interfere with the two top LVDT's on the left side of the wall. Those LVDT's were later re-positioned. Due to this, the imposed displacement history was divided into two intervals: one going from the start up to the 8mm cycles and the other one from the 8mm cycles to the final cycles. Later, the first interval was used to calibrate the numerical model and the second to conclude on the ability of the damage model to simulate adequately the wall's global behaviour.

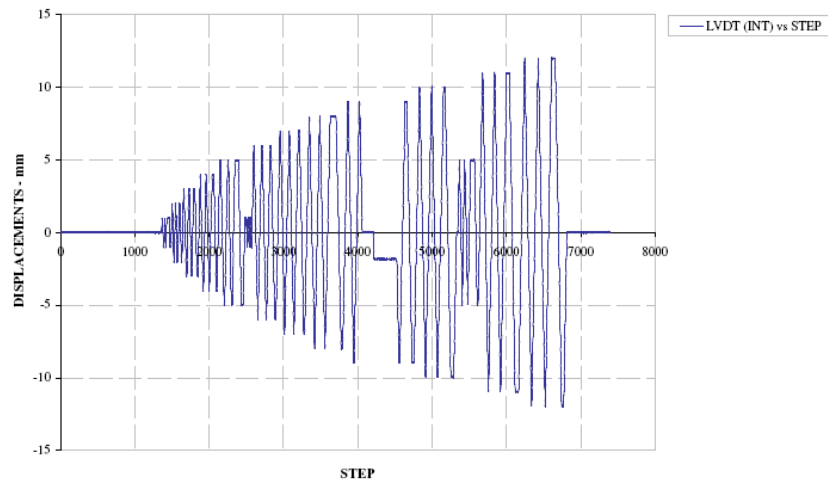


Figure 4: Total horizontal displacements vs Step.

## 2.3 Experimental test results

### 2.3.1 Analysis of the Force/Displacement response curve

Trough the analysis of the force/displacement experimental response curve (Figure 5), one can observe that:

- The tested masonry wall presents a medium energy dissipation capacity;
- The response is similar in both directions, although the final cycles, in particular the 11 and 12mm cycles, have shifted the response curve towards the positive direction of the displacements, meaning a tendency for positive plastics deformations at the end;
- The loading and unloading slopes present similar slopes;
- The loading stiffness of the structure remained almost constant during the whole test.

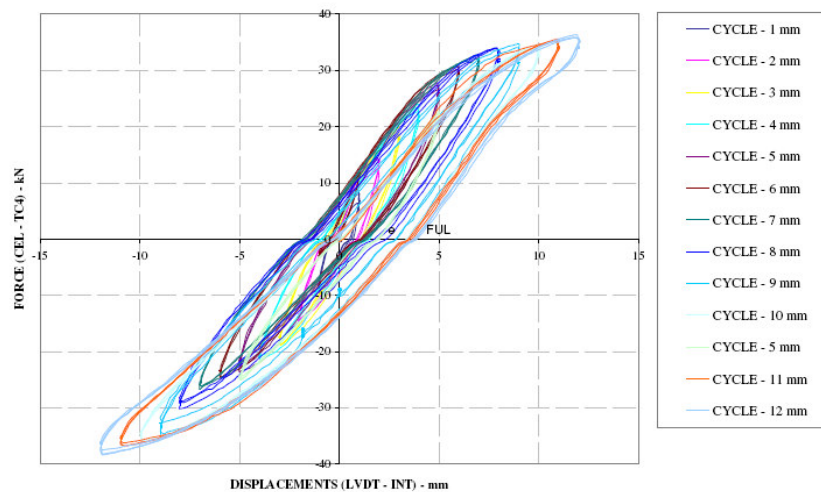


Figure 5: Horizontal top force vs Horizontal top displacement curve.

### 2.3.2 Analysis of the lateral joints behaviour

The behaviour of the lateral joints cannot be analysed separately, since the behaviour of one joint affects the others. Figure 6 shows the response of the lateral joints in terms of axial displacements (opening and closure) during the experimental test. Positive displacements correspond to opening of the joint while negative values are for joint closure.

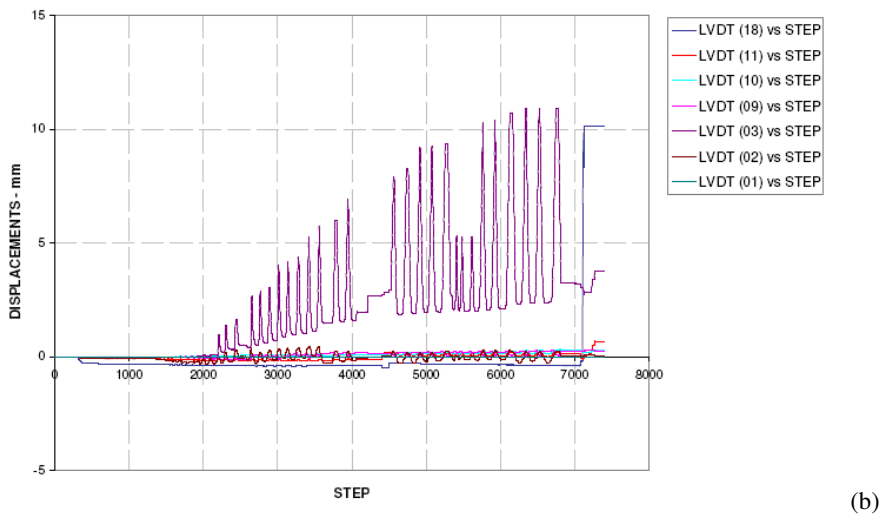
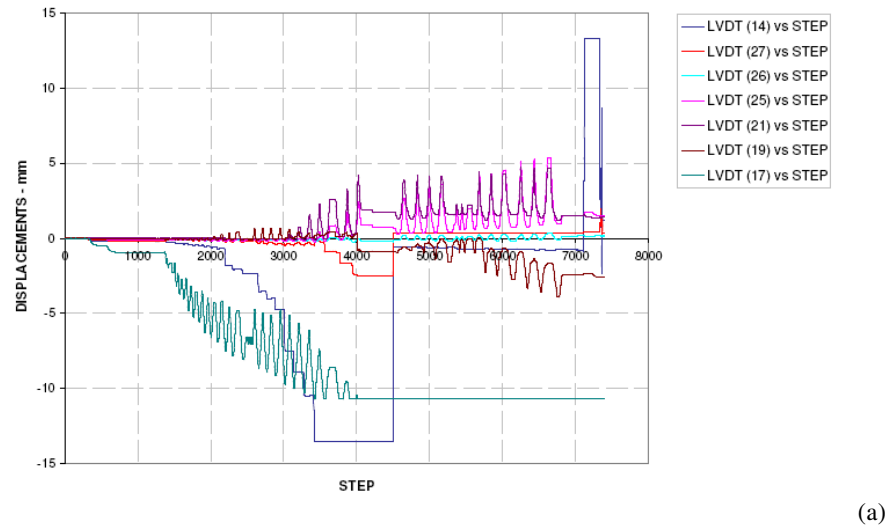


Figure 6: Joint behaviour vs Time history. (a) Left side. (b) Right side.

- Left side joints behaviour analysis:

The two monitored joints near the base, 17 and 19 (Figure 3), showed an overall tendency to close, especially the joint 17 in which the displacements exceeded the LVDT capability. This displacement was mainly due to the re-arrangement of the stones in the block foundation forced by the cyclic compression forces. On the other hand, the high stiffness of the foundation forced damage to be concentrated on the more fragile joints directly above (21 and 25) as it is shown in Figure 7 (a). These two joints presented progressive opening during the test. As

for the monitored joint 26, no particular displacement during the experiment test was observed.

The top monitored joints, 14 and 27, showed an unusual overall progression to close that was mostly connected to the lost of tension on the steel rods at the top of the wall, which interfered with the readings.

- Right side joints behaviour analysis:

The two monitored joints near the base, 01 and 02, showed almost no displacement during the experiment. This was mainly due to the high stiffness of the foundation, which forced the damage to be concentrated on the more fragile joint directly above (03). The graphic shows an important progressive opening during the test (Figure 7 (a)), meaning a considerable damage concentration at this joint.

The three monitored joints, 09, 10 and 11, directly above joint number 03 showed almost no displacement during the experiment. As for the monitored joint number 18 that corresponds to the LVDT at the top, it showed a slight tendency towards closure at the beginning. However near the step 7000 it presented a major opening, illustrated in Figure 7 (b), that exceeded the LVDT capability.

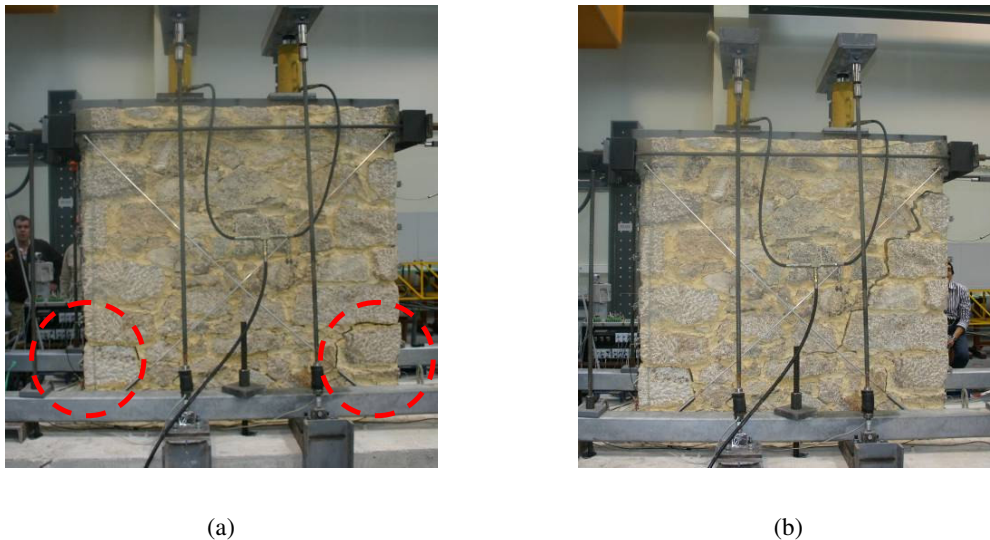


Figure 7: Damage concentration on the wall. (a) Damage concentration on base of the wall. (b) Damage on the top right side of the wall.

### 3 NUMERICAL SIMULATION

#### 3.1 Numerical model definition

The wall was simulated using the program Cast3M [1], a finite elements based computer code for structural analysis, that was developed by the French Commission for Atomic Energy (CEA). The Cast3M is a high-level tool for civil engineering investigation purposes and it integrates pre and post-processing functions (CEA, 2000). Since no discretization of the stones and joints was expected with the continuum damage model, only the external dimensions of the wall were needed to generate the finite elements mesh.

The mesh was constructed using auxiliary programs [10] that converted the geometry defined in Autocad [9] into the language gibiane (.dgibi) of Cast3M. The mesh is regular and made of 2x5x5 volumetric elements with 8 nodes (Figure 8).

In terms of constraints, the wall was considered to be fixed in the foundation block i.e. fixed at the base. In order to reproduce the experimental test, the same imposed vertical force and horizontal displacement histories were applied to the numerical model.

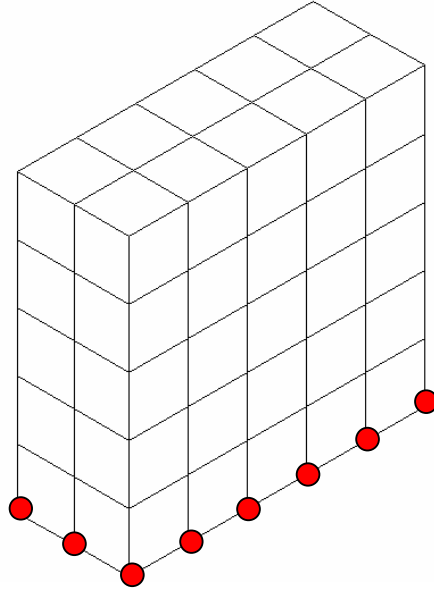


Figure 8: Numerical Model.

### 3.2 Main characteristics of the damage model

To better understand the damage model it is first important to understand the damage concept; it can be interpreted as a measure of several material parameters such as defects like micro-cracks and micro-cavities, associated to an internal surface element. The material non linearity is interpreted as the result of the evolution of those parameters [3].

The material constitutive laws were defined through a continuum damage model based on the continuum damage mechanics [3], originally developed for the analysis of large dimension concrete structures such as dams and capable of reproducing the dissimilar degrading phenomena that occur under tension or compression [4, 5]. This model incorporates two damage variables; one for tension ( $d^+$ ) and another for compression ( $d^-$ ) and a plastic deformation tensor for the characterization of the non-linear concrete degradation mechanisms under tensile and compression conditions.

The damage variables can only assume the values between 0 and 1 (1); 0 corresponds to elastic state, and increases with the evolution of the degradation until it reaches 1 that corresponds to the collapsed state.

$$0 \leq (d^+, d^-) \leq 1 \quad (1)$$

A basic entity of such a model is the “effective stress tensor” which is split into tensile and compressive components in order to clearly distinguish the respective stress contributions. According to the Coleman's relations the final constitutive law results in [5]:

$$\sigma = (1 - d^+) \bar{\sigma}^+ + (1 - d^-) \bar{\sigma}^- \quad (2)$$

The implemented damage model [6] depends of the following parameters:

Parameters	
EXTP	Reference strain for plastic parameter
STRP	Reference stress for plastic parameter
EXT1 EXT2	Extensions of two fitting points that belong to the material curve
STR1 STR2	Corresponding tensions of the fitting points
YOUN	Young module
NU	Poisson coefficient
RHO	Density
NCRI	Tensile softening criteria
FTUL	Tensile stress
REDC	Drop factor for peak tensile stress
FC01	Elastic limit compressive stress
RT45	Equi-biaxial compressive rate
EXTU	Ultimate limit strain
FCU1	Compressive peak stress
HLEN	Effective length
GVAL	Fracture energy

Table 1: Damage model parameters.

### 3.3 Damage model calibration

The continuum damage model, originally developed for concrete, is used in this work to simulate a stone masonry wall i.e., a quite heterogeneous element with anisotropic behaviour. Notice that the wall is made of stone and mortar filling in the spaces between stones, defining the joints.

In order to verify the ability of the model to simulate such masonry structure, the first and most important step is the calibration/comparison of the numerical results with the experimental curves. In the case of such a continuum model, only the global characteristics, such as the global stiffness (loading and unloading slopes) and the strength from the horizontal top force versus horizontal displacement behaviour curve will be foreseen. The local characteristics of the stones and the joints are indirectly considered and represented within the wall's global behaviour.

Therefore an optimization process was followed to minimize the deviation between the experimental and the numerical results. In order to better understand the influence of each damage model parameter (separately or together with others), a uni and multi-parametric analysis was performed. In the uni-parametric analysis, through the modification of each parameter it was possible to verify its influence on the material behaviour curve and on the wall's response curve. The values of the parameters were changed within acceptable intervals, although much higher or smaller values were tried in order to better understand the parameters influence.

Following the uni-parametric analysis, a multi-parametric analysis was performed having as reference the range of values from the uni-parametric study. In this analysis it was seen that

the effect caused by the alteration of one parameter didn't always stand when combined with the alteration of other parameters.

The numerical model was calibrated based on the experimental response on the top of the wall (horizontal force\ horizontal displacement curve) and taking into account the stiffness, the strength and the loading and unloading trajectories. Taking these aspects into account, and after an extensive iterative and optimization process, a good fit between the numerical and the experimental results was obtained for the values of the model parameters in Table 2.

Figure 9 presents the numerical response curve achieved using the values in Table 2, for a complete displacement cycle of 8mm.

Figure 10 illustrates the numerical cyclic tensile/compression axial stress-strain curve of a specimen made of the homogenous material that corresponds to the numerical results presented in Figure 9.

Parameters	Values	Units	Parameters	Values	Units
EXTP	-0.012	-	NCRI	1.0	-
STRP	-0.9	MPa	FTUL	0.05	MPa
EXT1	-0.003	-	REDC	0.05	MPa
EXT2	-0.008	-	FC01	-0.027	MPa
STR1	-0.16	MPa	RT45	1.18	-
STR2	-0.12	MPa	EXTU	-0.1	-
YOUN	9.5e7	Pa	FCU1	-15	MPa
NU	0.3	-	HLEN	0.3	m
RHO	2500	Kg/m <sup>3</sup>	GVAL	200	J

Table 2: Calibrated values.

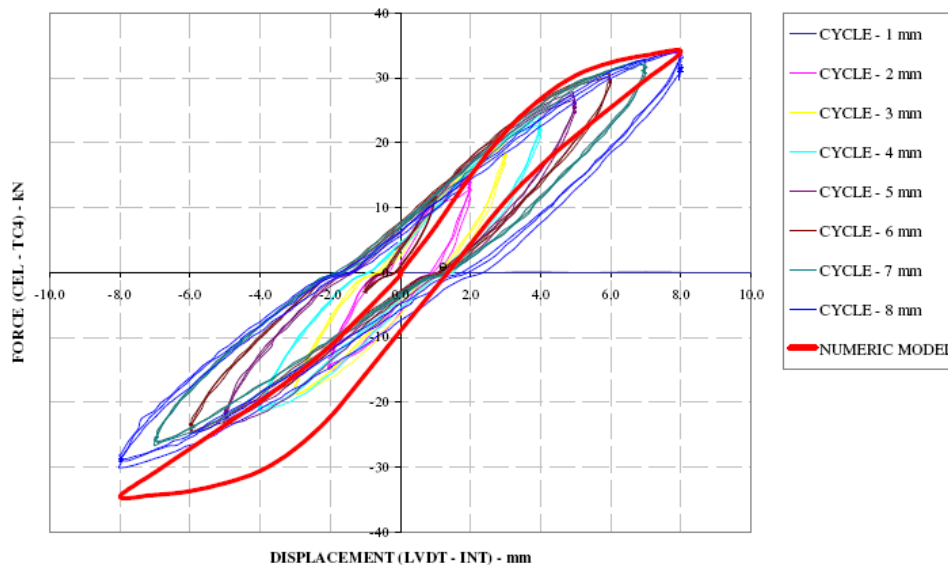


Figure 9: Numerical adjustment curve.

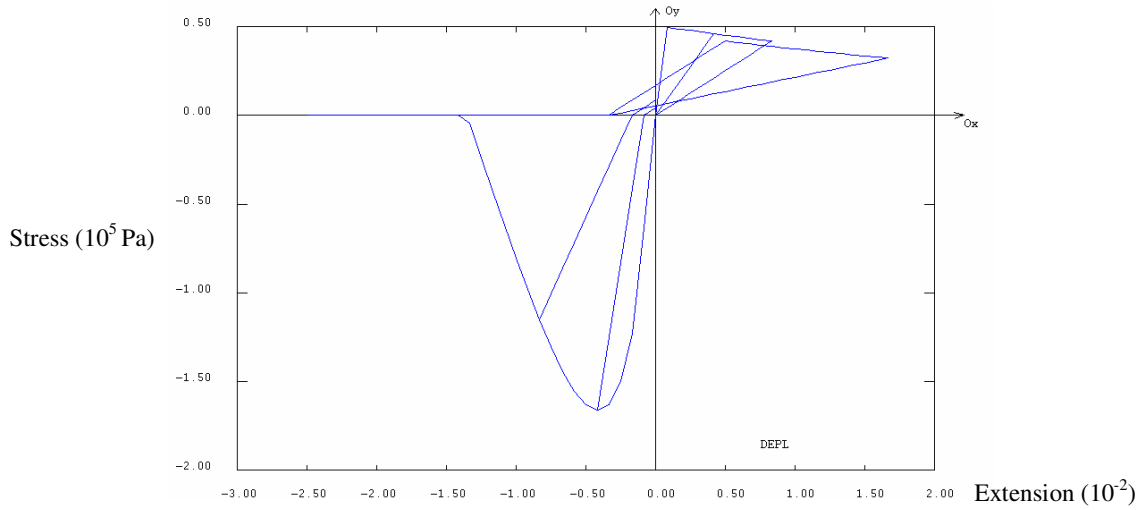


Figure 10: Material behaviour law.

Figure 11 presents the principal stresses ( $\sigma_{11}$  and  $\sigma_{zz}$ ) for the maximum displacement imposed (12mm) in both directions.

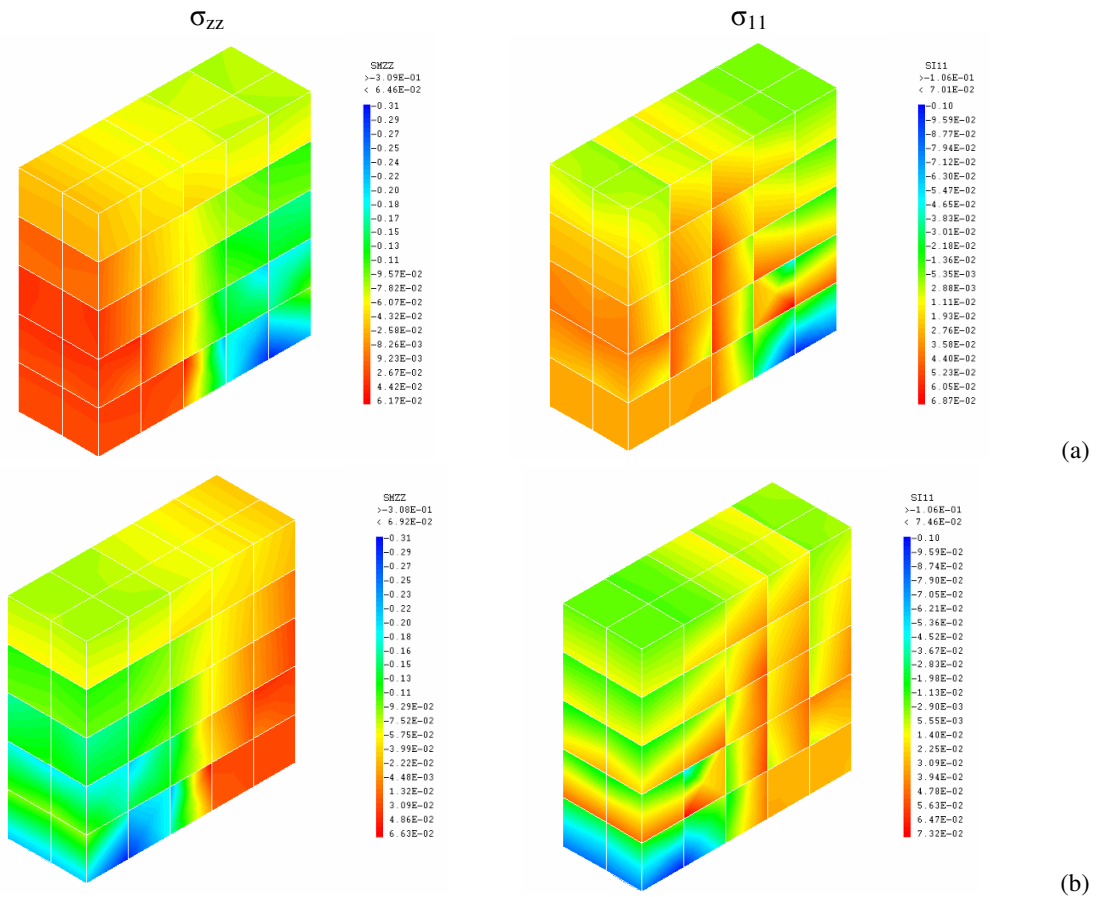


Figure 11: Main stress  $\sigma_{zz}$  and  $\sigma_{11}$  (MPa) for the maximum displacement in both directions: (a) 12mm. (b) -12mm.

For the maximum displacement (12mm) in both directions, it is possible to verify (Figure 11) an almost complete symmetry for the stresses in both principal directions. It is also possi-

ble to observe the main areas of damage near the base in both sides of the wall as shown in Figure 7 (a).

#### 4 CONCLUSIONS - NUMERICAL MODEL VS EXPERIMENTAL RESULTS

A stone masonry wall was built and tested at the Laboratory of Seismic and Structural Engineering at FEUP and a continuum damage model was used to simulate the response. Using the parameter's values from the model calibration, the numerical curve for the full time history of the experiment was obtained and compared to the corresponding experimental curve (Figure 12). The model allowed achieving a good fitting in terms of strength and initial stiffness for the global horizontal force versus horizontal in-plane displacement curve. Notice that this study did not involved the evaluation of the stone masonry wall characteristics using the numerical model, but the numerical simulation of an experiment in order to verify the ability of the model to represent, in a global way, the behaviour of such structure.

However some difficulties were encountered when using this model, mainly because it is a model comparable to a smeared crack model that is unable to capture phenomena like friction, related to the local joint behaviour. In particular, the comparison between the numerical results expressed in Figure 9 for only one cycle (8mm), and the one for the full time history in Figure 12, showed that for the same level of displacement the structure in the second case presents a less plastic and, apparently, dissipative behaviour. This occurred due to the progressive tensile damage induced by the intermediate cycles which forced a higher tensile damage when compared to the single cycle response. This effect imposed a decrease on the stiffness, particularly visible on the unloading curves that for the full time history pointed to the origin, inducing a less dissipative elastic behaviour. Therefore, when compared to the experimental results, the continuum damage model didn't represent in a very accurate way the loading and unloading stiffness and, consequently, the energy dissipation for larger displacements imposed to the structure. Throughout the calibration process, the adjustment of the model parameters didn't allow overcoming this aspect.

Pursuing this type of continuum models for masonry structures, new developments are being followed in order to solve the encountered difficulties, especially to provide a higher energy dissipation capacity, an aspect that is particularly important when cyclic/dynamic actions are involved.

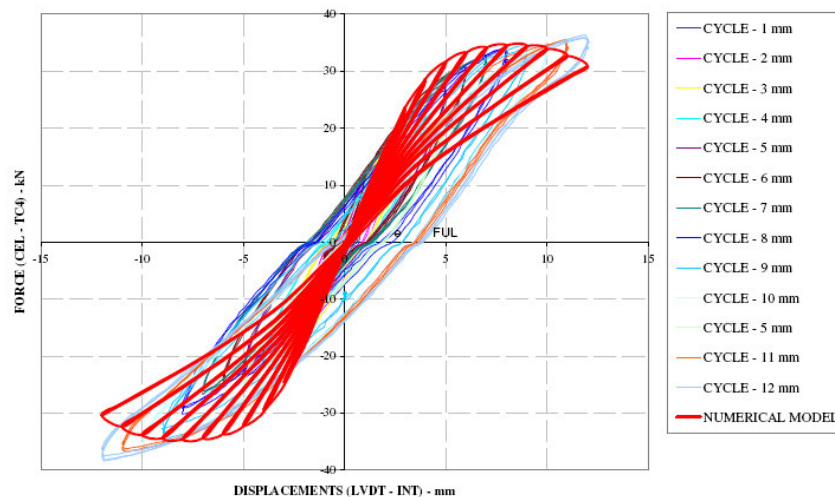


Figure 12: Experimental response curve vs Numerical response curve.

## REFERENCES

- [1] Commissariat à l'Énergie Atomique; *P. Pasquet, Manuel d'utilisation de Cast3M*, [www.cast3m.cea.fr](http://www.cast3m.cea.fr), 2003.
- [2] Faria R., *Avaliação do comportamento Sísmico de Barragens de Betão através de um Modelo de Dano Contínuo*, PhD Thesis. FEUP, 1994.
- [3] Faria, R., Nelson V. P., Delgado R., *Simulation of the cyclic behaviour of R/C rectangular hollow section bridge piers via a detailed numeric model*, Journal of Earthquake Engineering, Vol. 8, No. 5, Imperial College Press, 2004.
- [4] Faria, R. and Oliver, J., *A Rate Dependent Plastic-Damage Constitutive Model for Large Scale Computations in Concrete Structures*, CIMNE Monograph N.17, Barcelona, 1993.
- [5] Faria, R., Oliver, J. and Cervera, M., *A strain-based plastic viscous-damage model for massive concrete structures*, International Journal of Solids and Structures 35 (14), 1533 - 1558, 1998.
- [6] Costa C., Pegon P., Arêde A., Castro J., *Implementation of the Damage Model in Tension and Compression with Plasticity in Cast3M*, 2004.
- [7] Costa A. A., Silva B., Costa A., Guedes J., Arêde A., *Structural behaviour of a masonry wall under horizontal cyclic load; experimental and numerical study*, Structural Analysis of Historical Constructions, New Delhi, 2006.
- [8] Lourenço P. B., *Computer strategies for masonry structures*, Deft University Press, 1996.
- [9] AutoCAD, Autodesk. <http://www.autodesk.pt/>, 2006.
- [10] GiD, *International Center for Numerical Methods and Engineering*, <http://gid.cimne.upc.es/>, 2006.